APPENDIX A

FIGURES

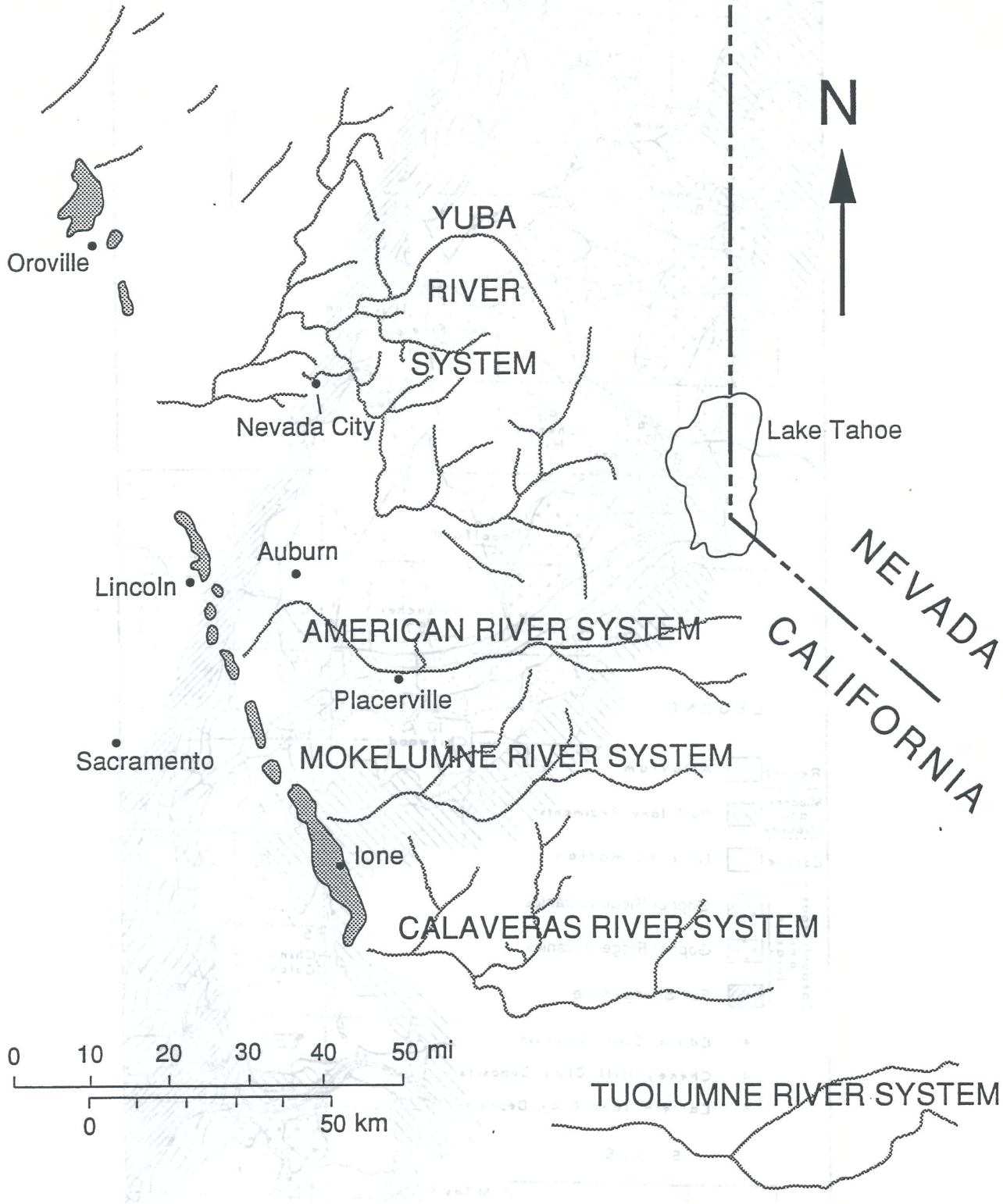

Figure 1

Ione depositional system including Ione Fm. outcrops and Early Tertiary channels. (adapted from Clark, 1965; Bateman and Wahrhaftig, 1966)

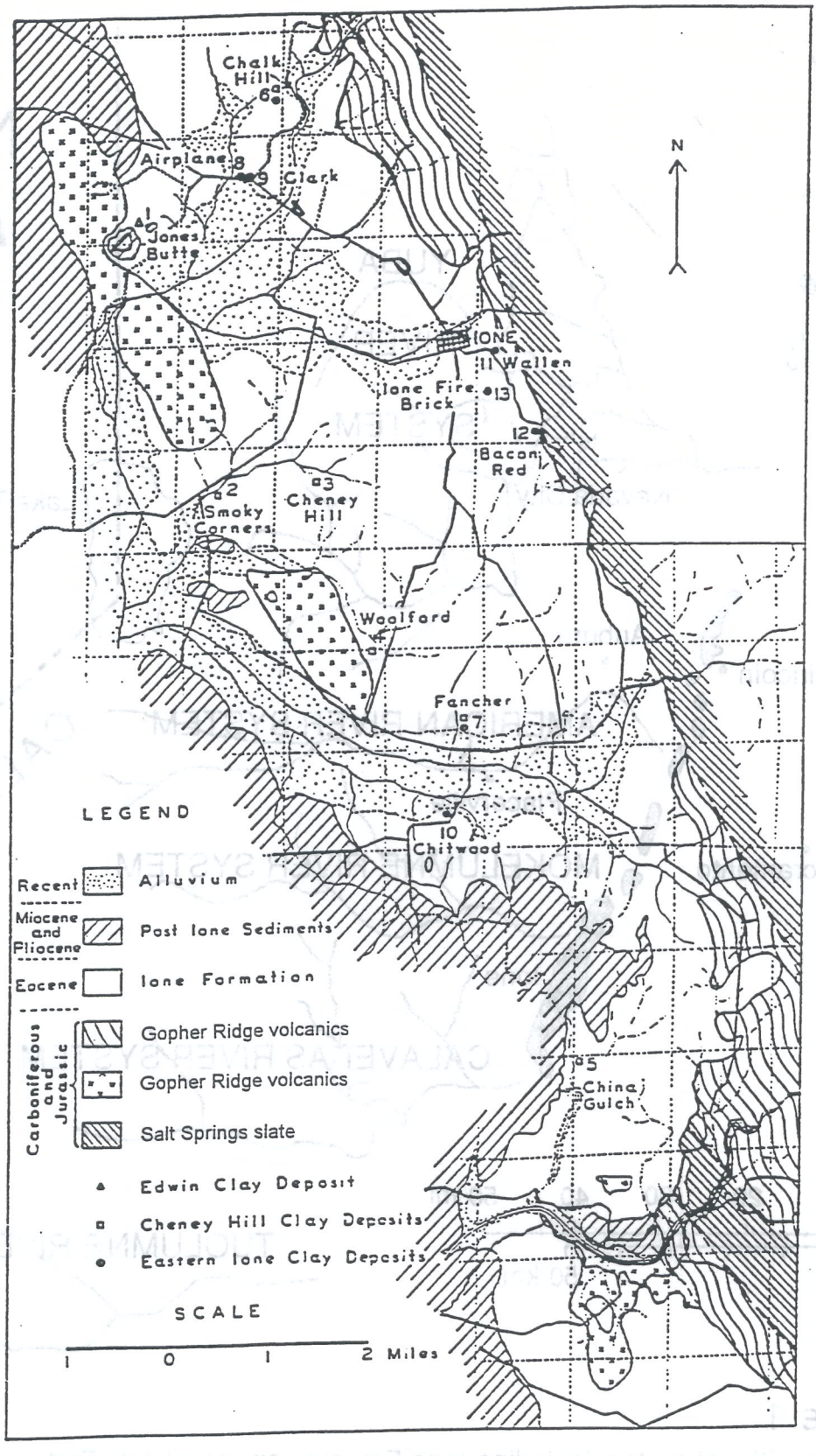

Figure 2 Geologic map of the Ione area. (modified from Bates, 1945)

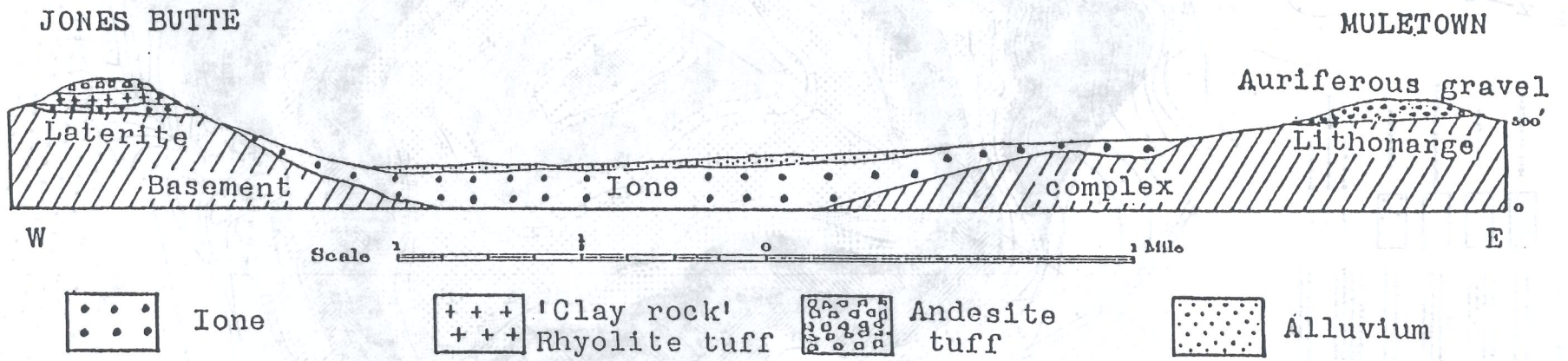

Figure 3

Schematic cross-section across the Ione Valley. "Lithomarge" is equivalent to the term "saprolite" (from Allen, 1929).

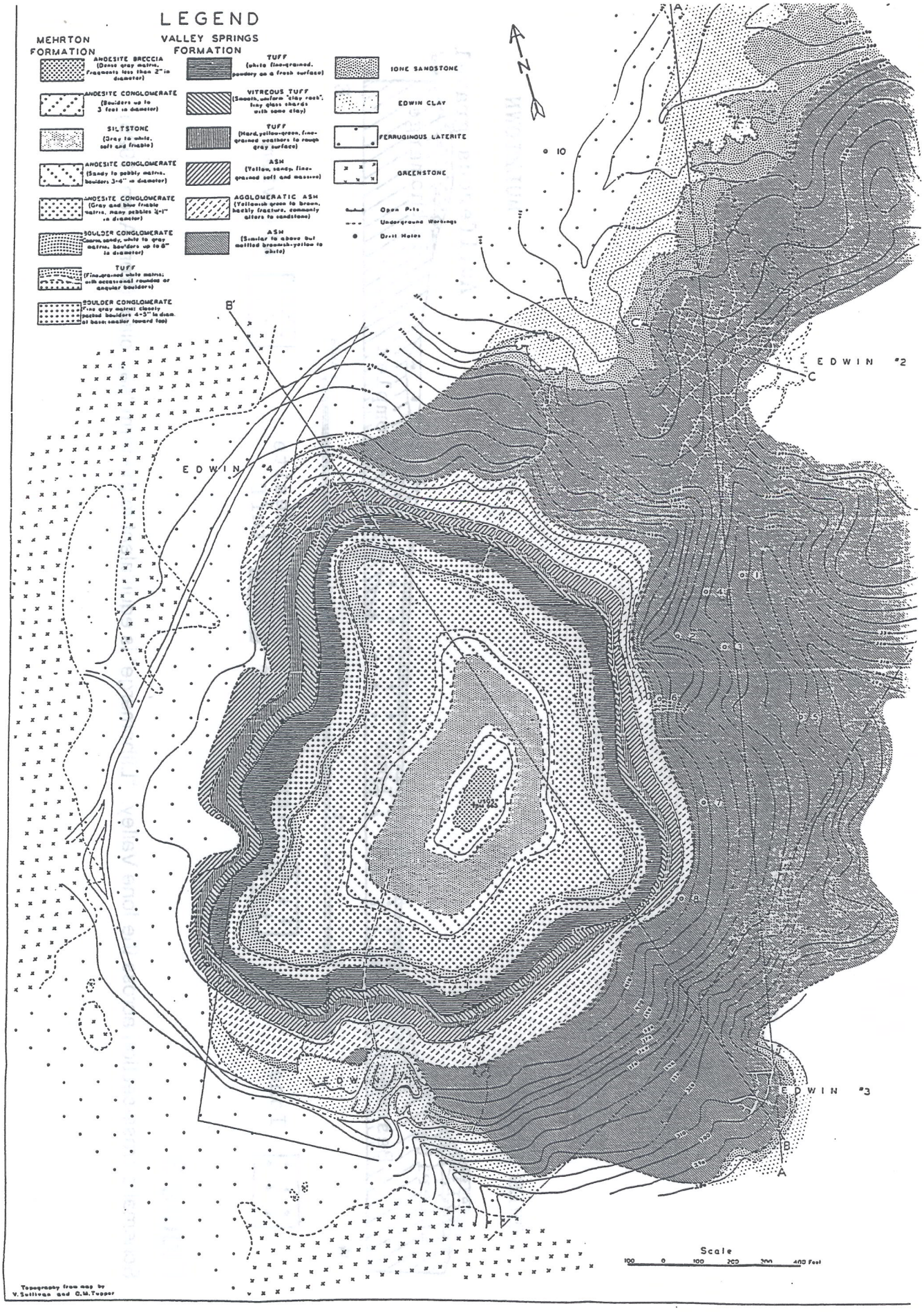

Figure 4a Geologic map of the Jones Butte area. (from Bates, 1945)

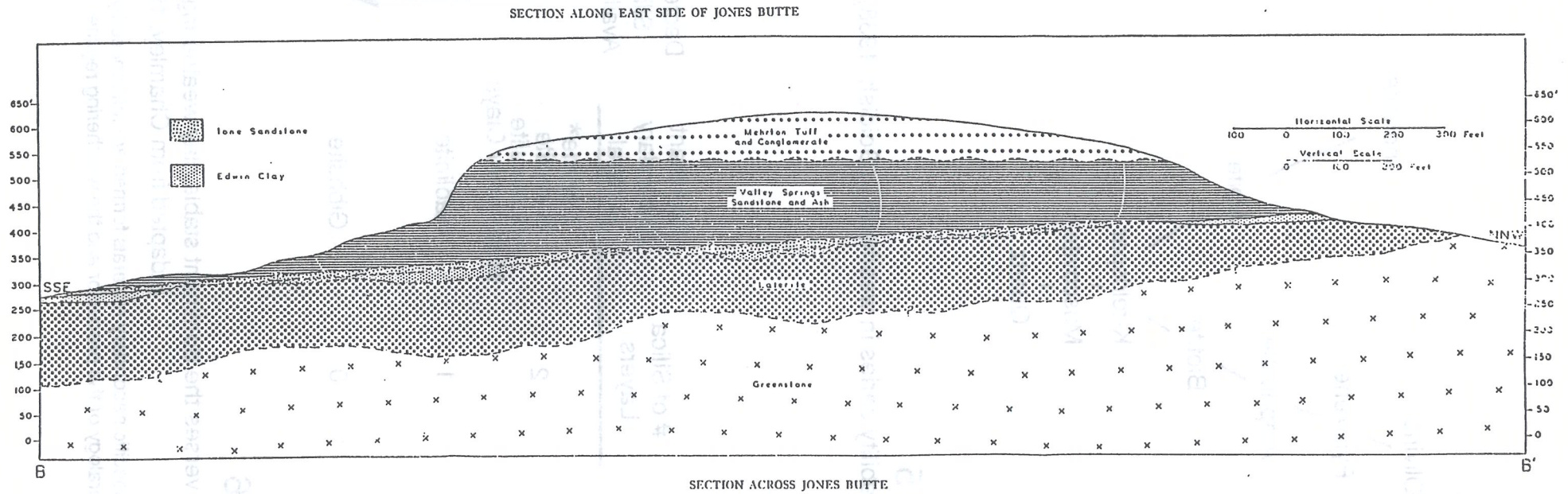

Figure 4b Cross-section **B–B′** from map, Figure 4a.

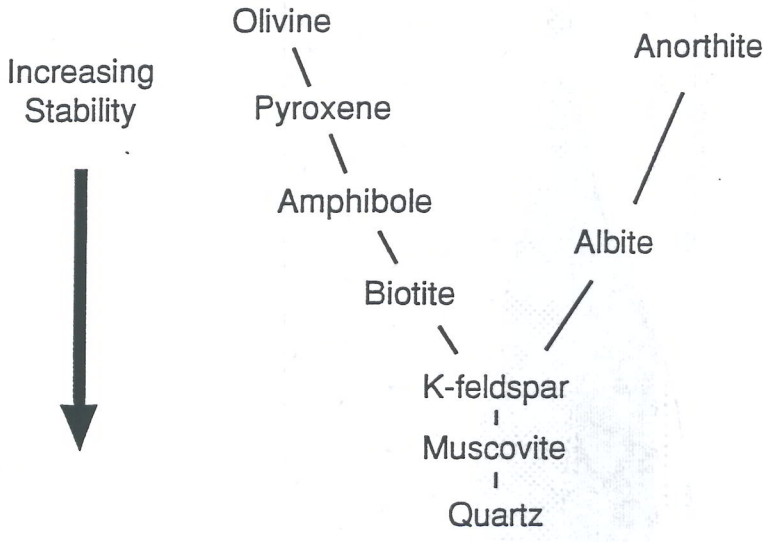

Figure 5
Mineral stability series in weathering (Goldish, 1938).

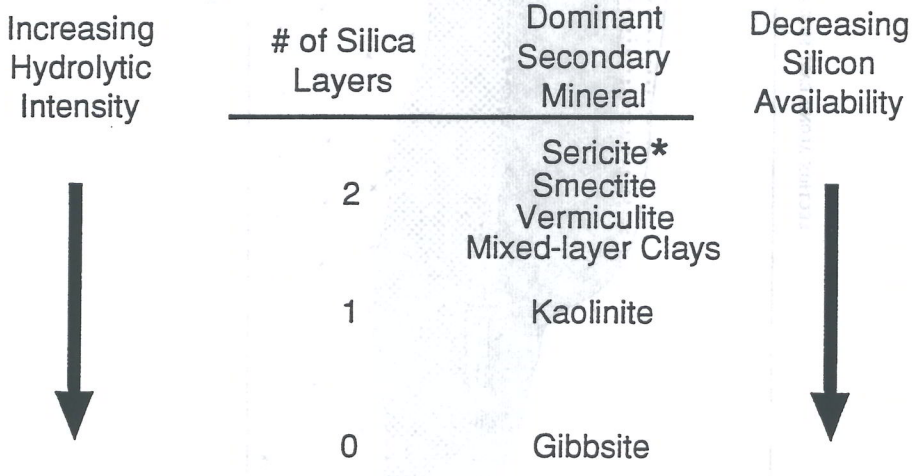

Figure 6
Hydrolysis verses the dominant stable clay weathering product.
(adapted from Chamley, 1989)

* Note: the specific secondary minerals formed are influenced by the mineralogy of the precursor and the weathering regime.

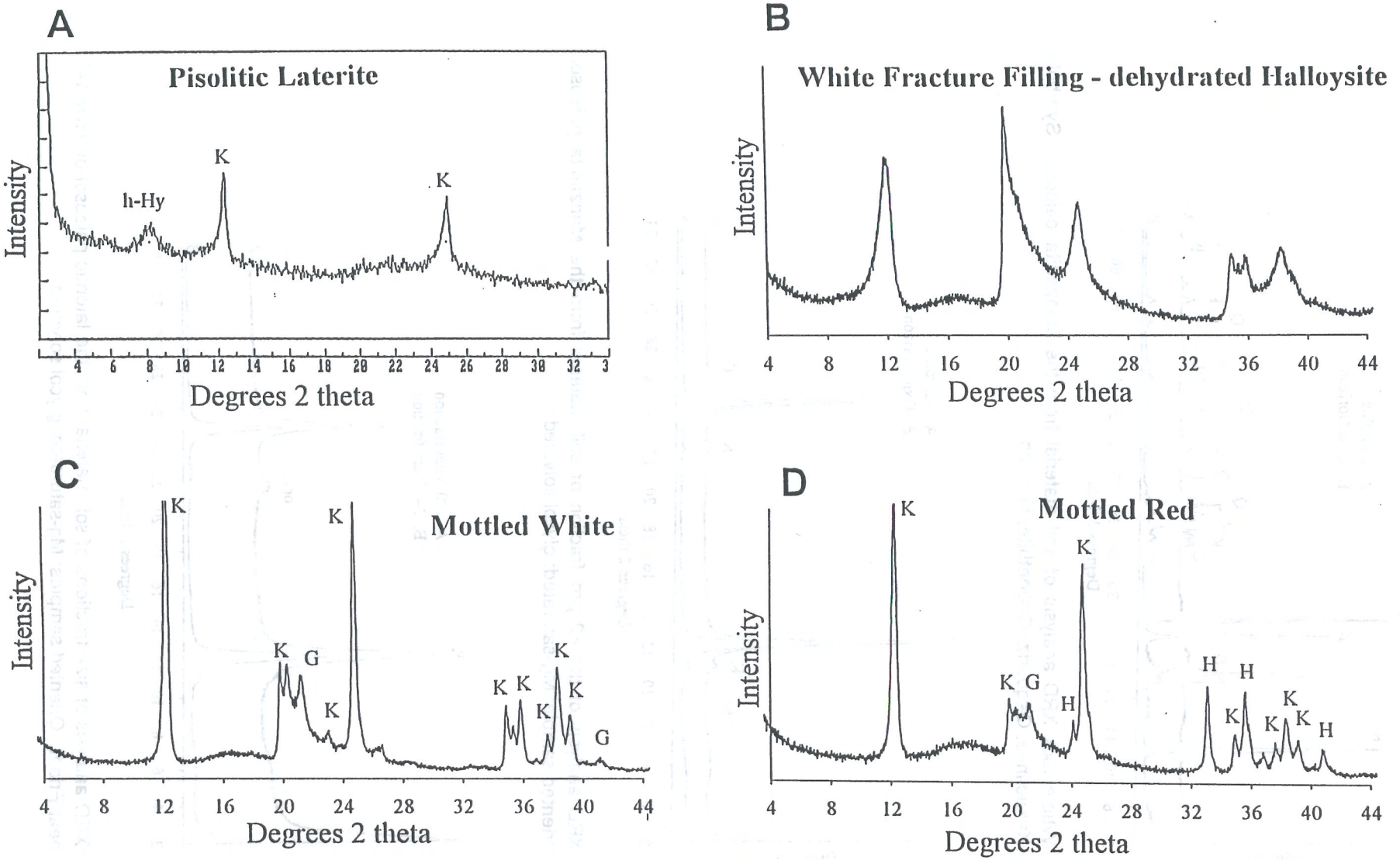

Figure 7

X-ray diffraction analyses of altered material from the lateritic paleosol at Jones Butte. **A.** <0.5 μm fraction of pisolitic material. Oriented sample; Mg-saturated; glycol-solvated. **B-D.** Whole rock XRD - randomly packed powder mounts. Symbols: K = kaolinite, G = goethite, H = hematite, h-Hy = hydrated halloysite.

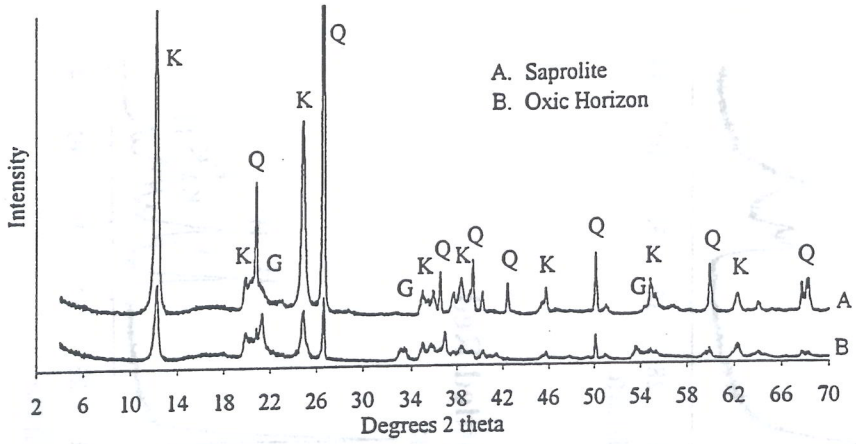

Figure 8. Whole rock XRD analysis of soil material from the Manzanita paleosol. Symbols: K=kaolinite, Q=quartz, G=goethite, M=mica.

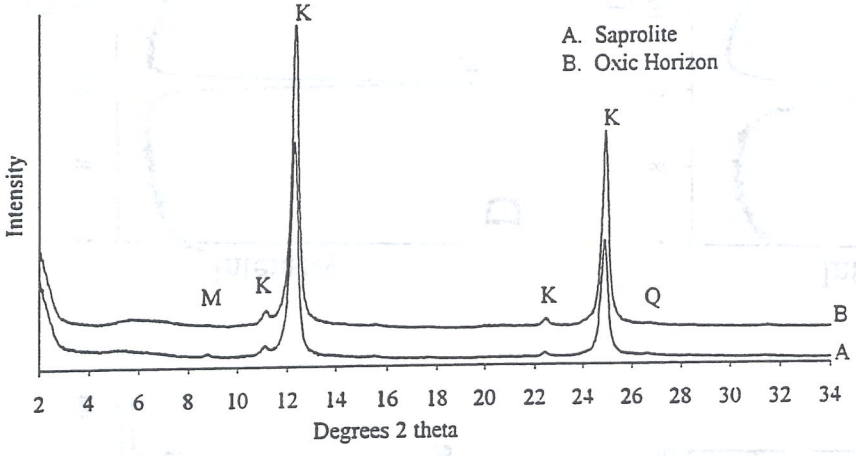

Figure 9. XRD analysis of the <2 μm fraction of soil material from the Manzanita paleosol. Oriented sample; Mg-saturated; glycol solvated.

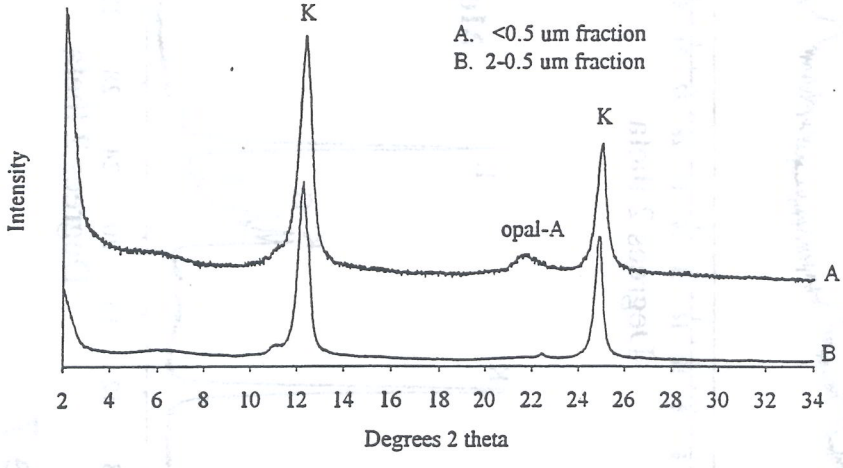

Figure 10. XRD analysis of size fractions of soil material from the lateritic paleosol on Hwy 145 near Friant. Oriented samples; Mg-saturated; glycol solvated.

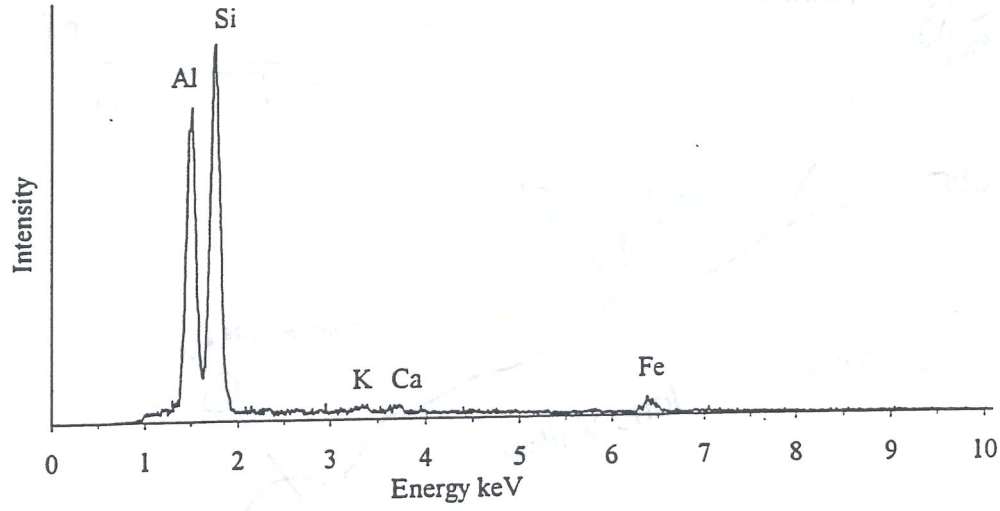

Figure 11. EDX analysis of kaolinite with siliceous cement coating in the saprolite of the Manzanita Oxisol, Nevada City.

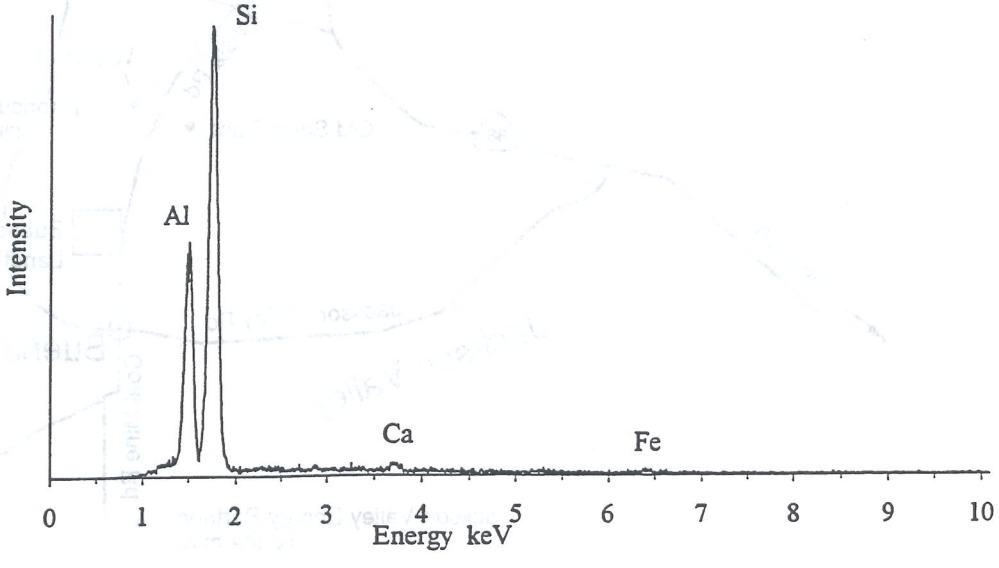

Figure 12. EDX analysis of kaolinite with siliceous cement in the saprolite of the lateritic paleosol on Hwy 145 near Friant (north of Fresno).

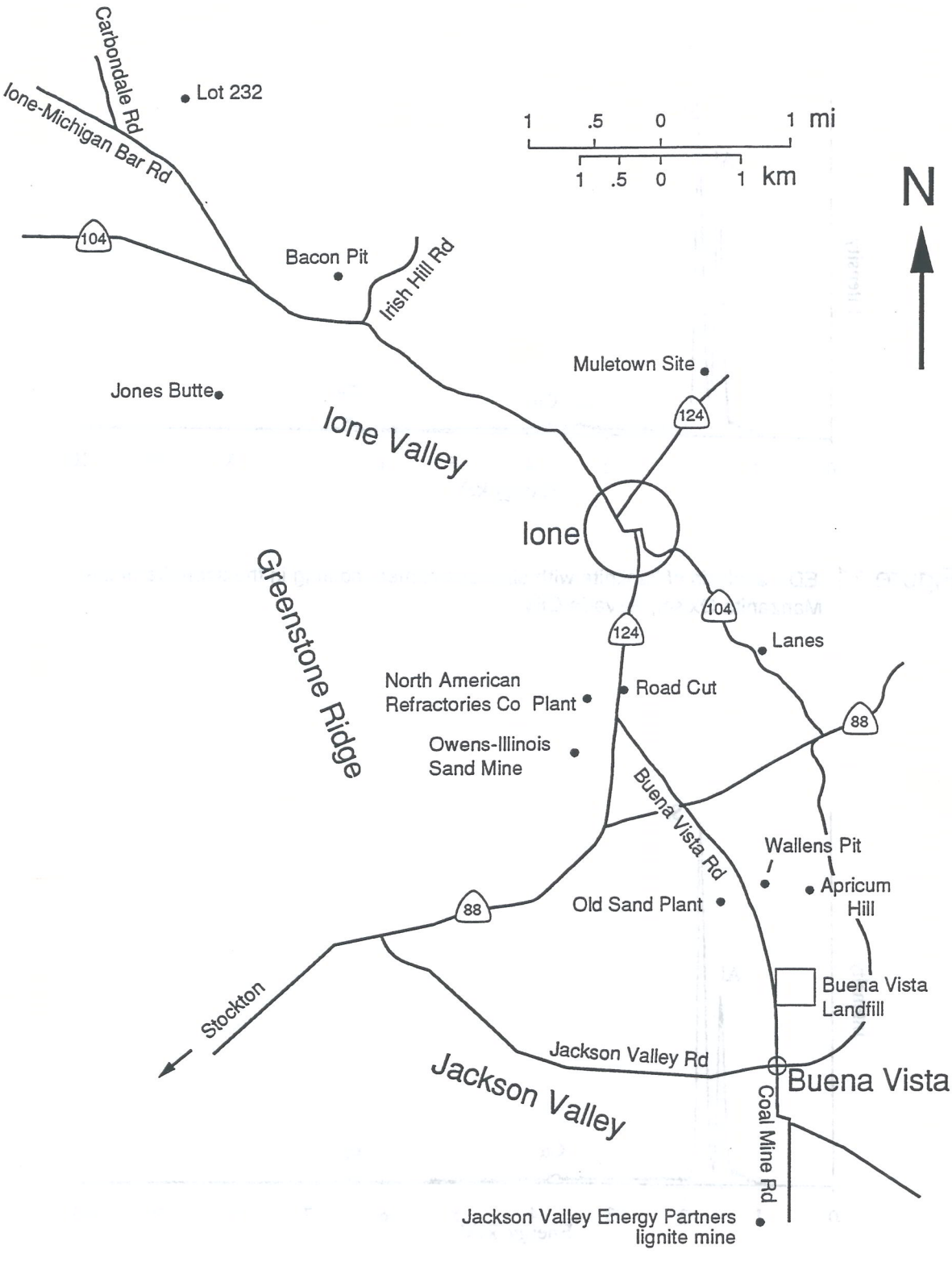

Figure 13
Sample localities and field trip stops in the Ione area.
Lot numbers refer to Arroyo Seco Ranch subdivisions.

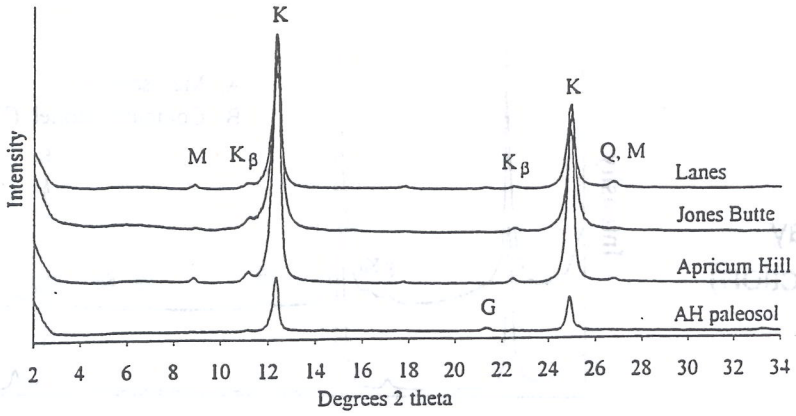

Figure 14. XRD analysis the of the <2 µm fraction of representative lower Ione sandstones across the Ione Valley (Mg-glycol treatment). Symbols: K=kaolinite, Q=quartz, G=goethite, M=mica.

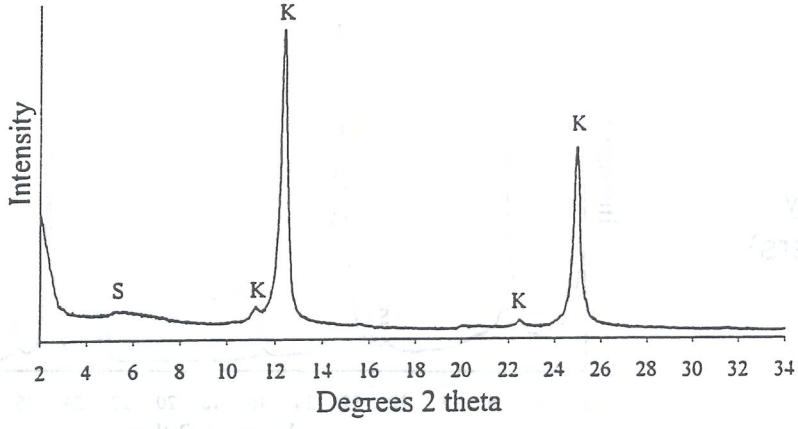

Figure 15. XRD analysis of the <2 µm fraction of the Edwin Clay at Jones Butte. Oriented sample; Mg-saturated; glycol solvated. S = smectite.

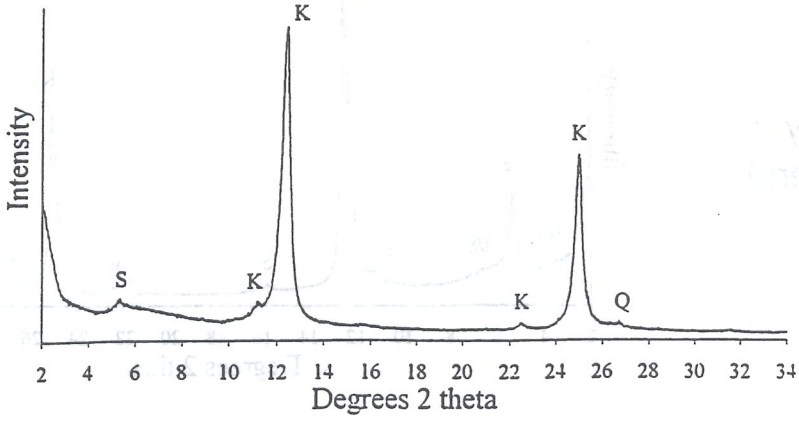

Figure 16. XRD analysis of the <2 µm fraction of B6 clay from the Bacon Pit. Oriented sample; Mg-saturated; glycol solvated.

a. M21 clay
(top of section)

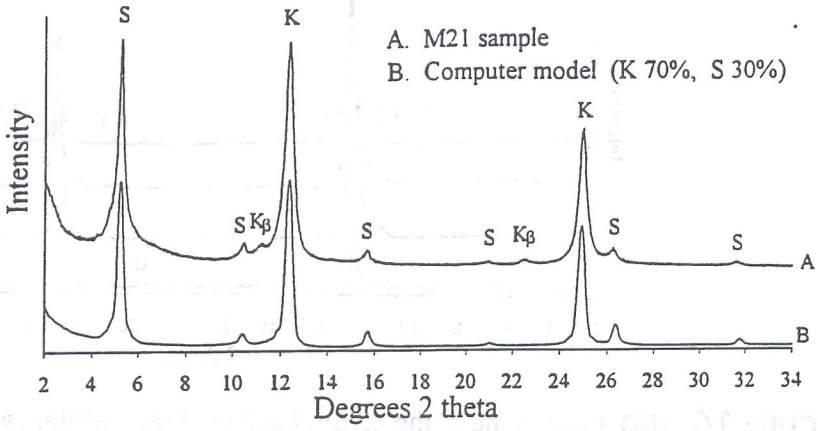

b. B2 clay
(– 5 meters)

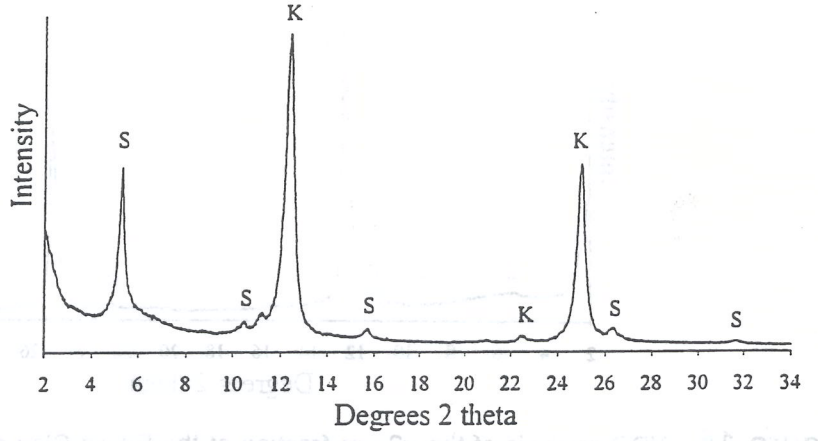

c. B3 clay
(– 7 meters)

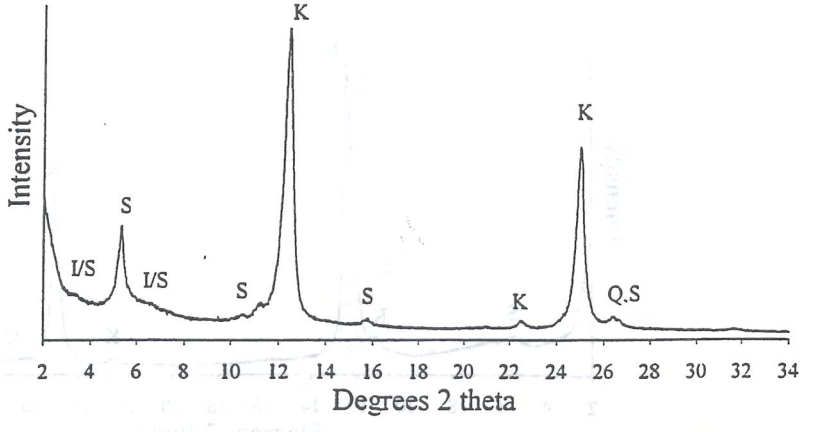

Figure 17. XRD analysis of the <2 μm fraction of M21 (a), B2 (b) and B3 (c) clays from the Bacon Pit. Oriented sample; Mg-saturated; glycol solvated. K = kaolinite, S = smectite, I/S = illite/smectite mixed-layered clay.

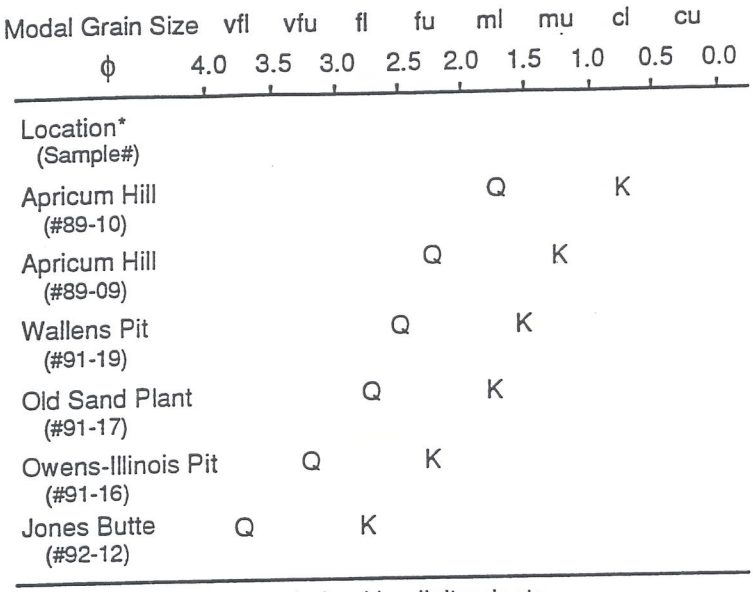

Figure 18. Grain size relationship of quartz grains and detrital clay clasts in lower Ione sandstones in the Ione area. (from Wood, 1994)

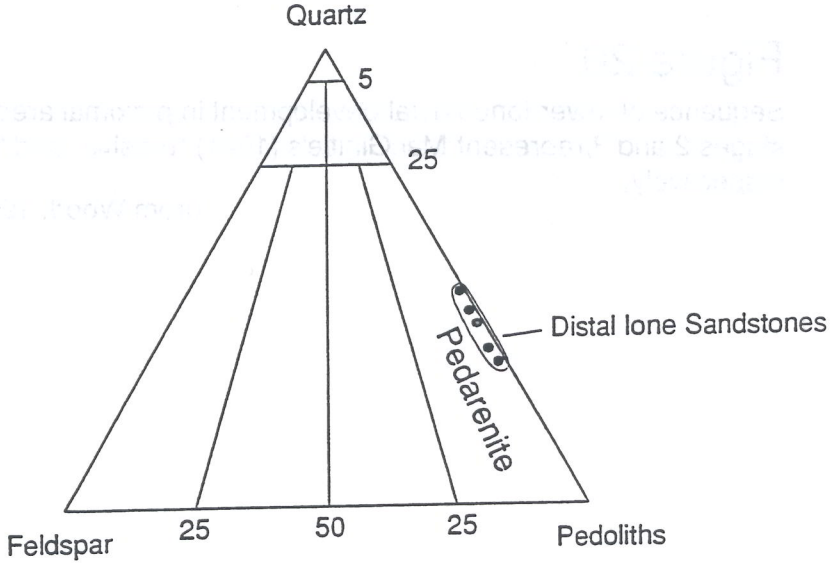

Figure 19. Compositions of lower Ione sandstones in the Ione area in the Folk (1974) classification scheme. (from Wood, 1994)

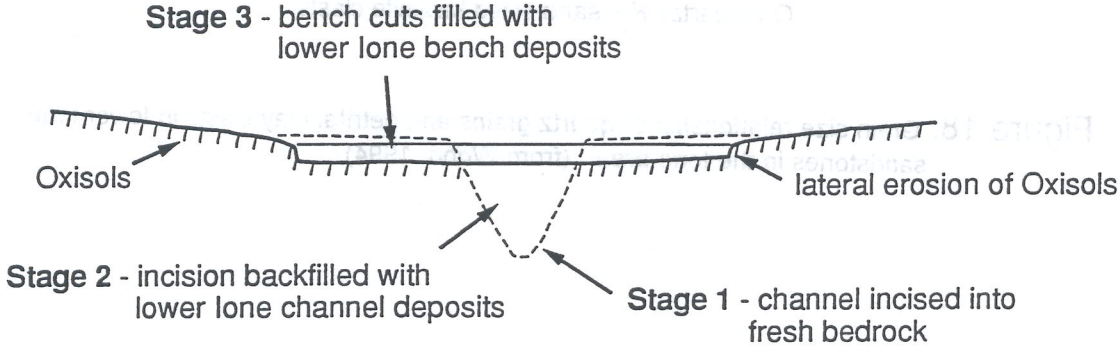

Figure 20

Sequence of lower lone fluvial development in proximal areas. Stage 1 and stages 2 and 3 represent MacGinitie's (1941) "erosive" and "aggradation stages", respectively.

(from Wood, 1994)

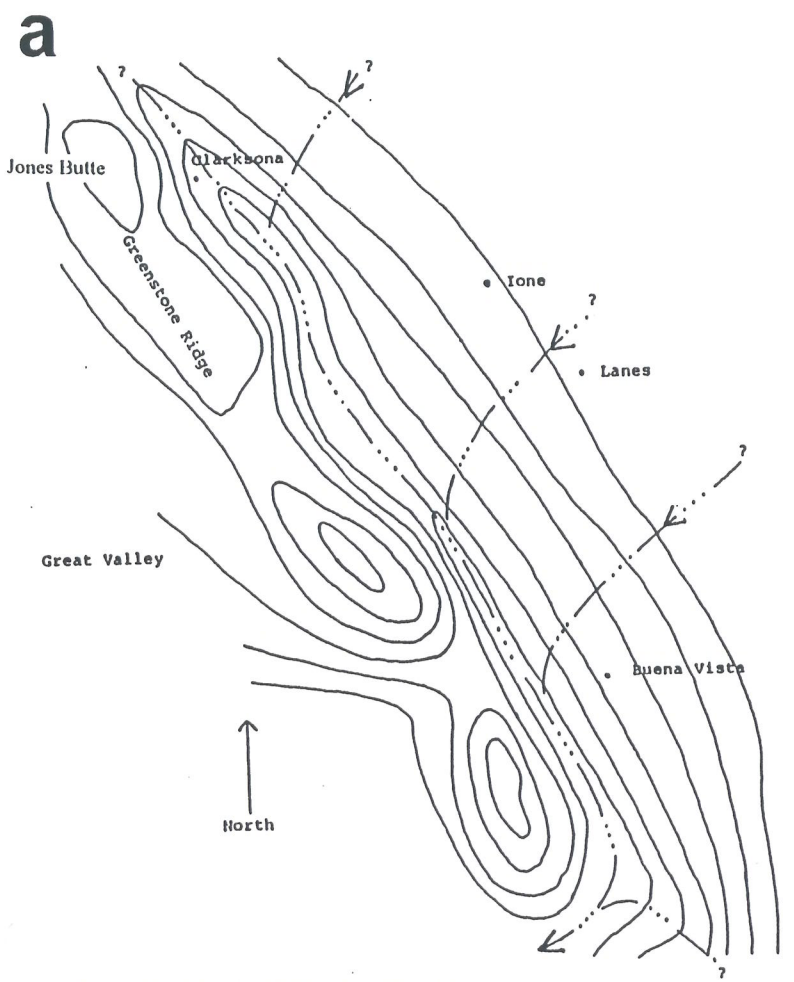

(from Rodgers, 1986–modified from Chapman and Bishop, 1975)

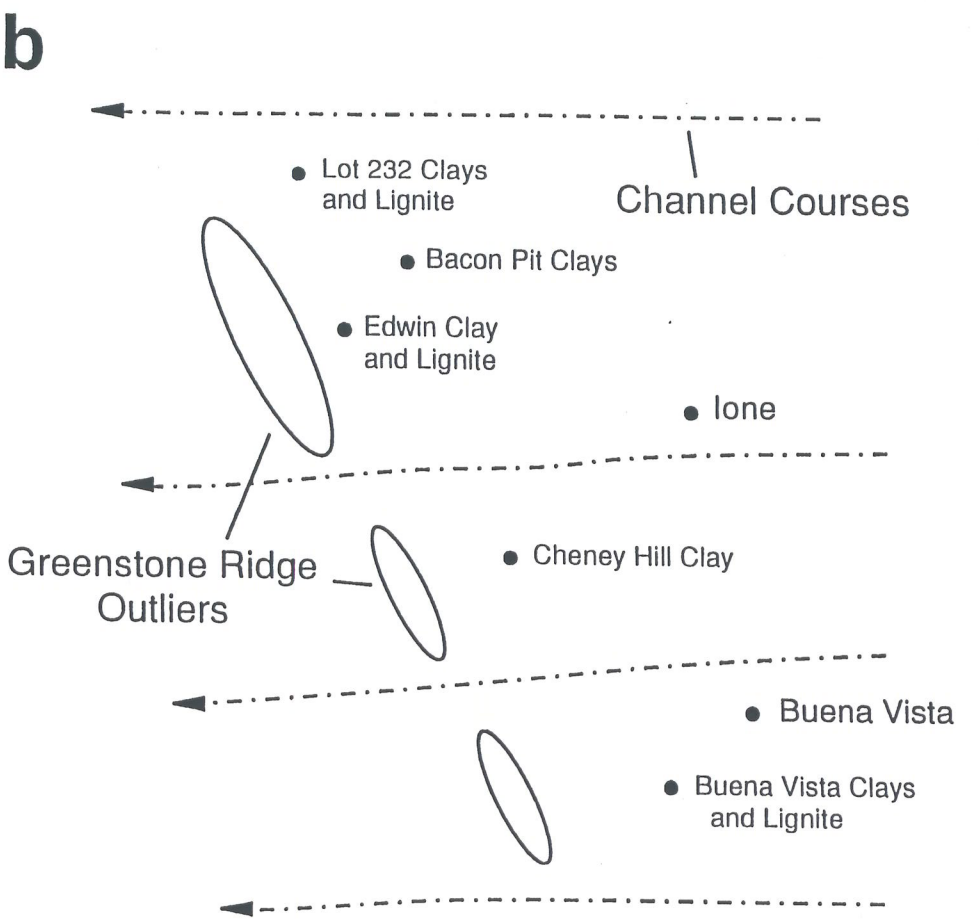

(adapted from Rodgers, 1986)

Figure 21. Paleogeography at the beginning (**a**) and end (**b**) of lower Ione deposition with the locations of some important clay and lignite deposits.

APPENDIX B

PHOTOMICROGRAPHS

Key to abbreviations used in descriptions of photomicrographs:

BSE	back scattered electron mode—microprobe
PPL	plane polarized light—optical microscope
WRL	white reflected light—optical microscope
BRL	blue reflected light—fluorescence microscope
O-F	opaque-fluorescent cement (PPL & BRL)
P-F	pale-fluorescent cement (PPL & BRL)

Photo 1. Saprolite (#90-06B), Coyote Rd, Nevada City (PPL). View shows the granitic saprolite fabric comprised of quartz (white), kaolinized mica books (KM), zircon (Z), domains of coarse-grained kaolinite with vermicular morphologies (a), domains of fine-grained massive kaolinite (b), and a network of packing voids (c). O-F cement (black) saturates kaolinized mica and O-F particulate morphologies are associated with the coarser grained kaolinite (a) and at lower left of photo.

Photo 2. Saprolite (#90-07), Coyote Rd, Nevada City (BRL). View shows zone of kaolinite fabric saturated by P-F cement (yellow). Kaolinite fabric surrounding cemented zone is impregnated with non-fluorescent blue epoxy (blue-gray). Adjacent quartz grains appear black. P-F cement also fills fractures in quartz grains in the saprolite fabric and appears yellowish orange in the photo.

Photo 3. Ione sandstone (#91-17), Old Sand Plant, Ione (PPL). View shows well-sorted, bimodal, fine- to medium-grained kaolinitic sandstone. Hydrodynamically equivalent quartz and detrital clay clasts comprise the sandstone fabric. K-feldspar (K) and heavy minerals including amphibole (A) occur in trace amounts. Little post-depositional compaction has occurred and quartz cement is absent. The clay aggregates are concentrated in a larger modal grain size compared to quartz because of their inherent microporosity and lower bulk density. The occurrence of larger clay aggregates results in "gaps" in the sandstone fabric. The clay aggregates form pseudomatrix as result of deformation between rigid framework grains. Adjacent clay aggregates exhibit drastic variations in microfabrics ranging from fine-grained massive kaolinite (a) to coarse-grained kaolinite with vermicular morphologies (b). Clay aggregates commonly possess remnant O-F cement coatings (c). Amphibole grains show no signs of post-depositional weathering.

Photo 4. Ione sandstone (#91-17), Old Sand Plant, Ione (BSE). View shows typical fabric of well sorted Lower Ione sandstones. Three detrital kaolinite aggregates with dramatically different microfabrics were deformed by impinging quartz grains (beige) and formed pseudomatrix. Heavy minerals (bright white) occur in a slightly smaller modal grain size than quartz and are commonly concentrated along laminae. The boundaries of adjacent clay aggregates are distinguished by an abrupt change in microfabric (a). The boundaries of clay aggregates with primary pores are commonly marked by a meniscus which drapes between quartz grains (b). The image shows the grain size difference between quartz and hydrodynamically equivalent detrital clay aggregates of lower density. The squashed clay aggregates form "gaps" in the sandstone fabric.

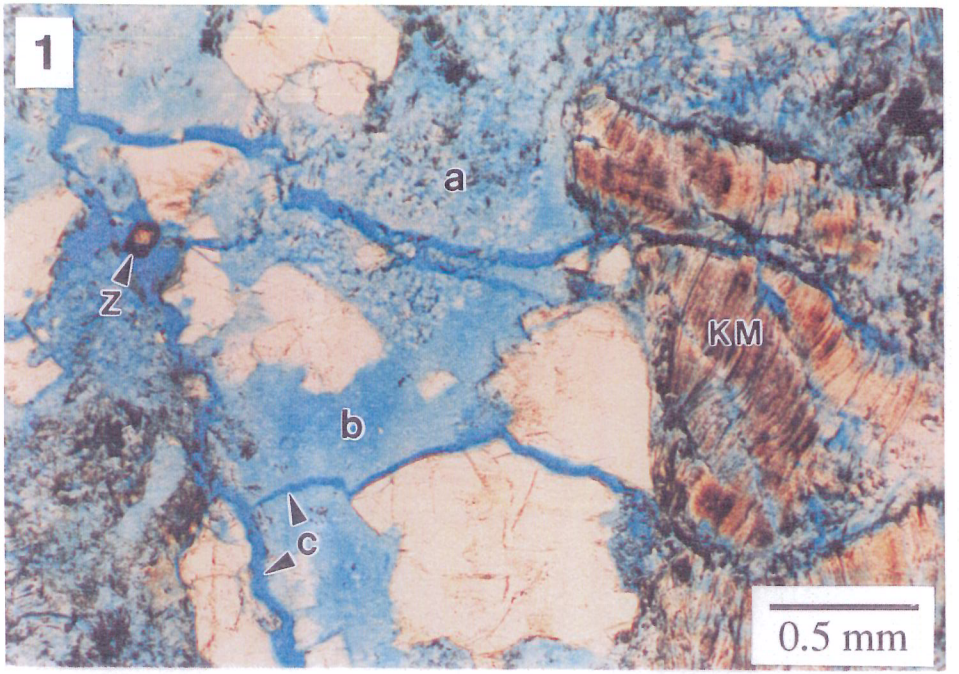
1
a
Z
KM
b
c
0.5 mm

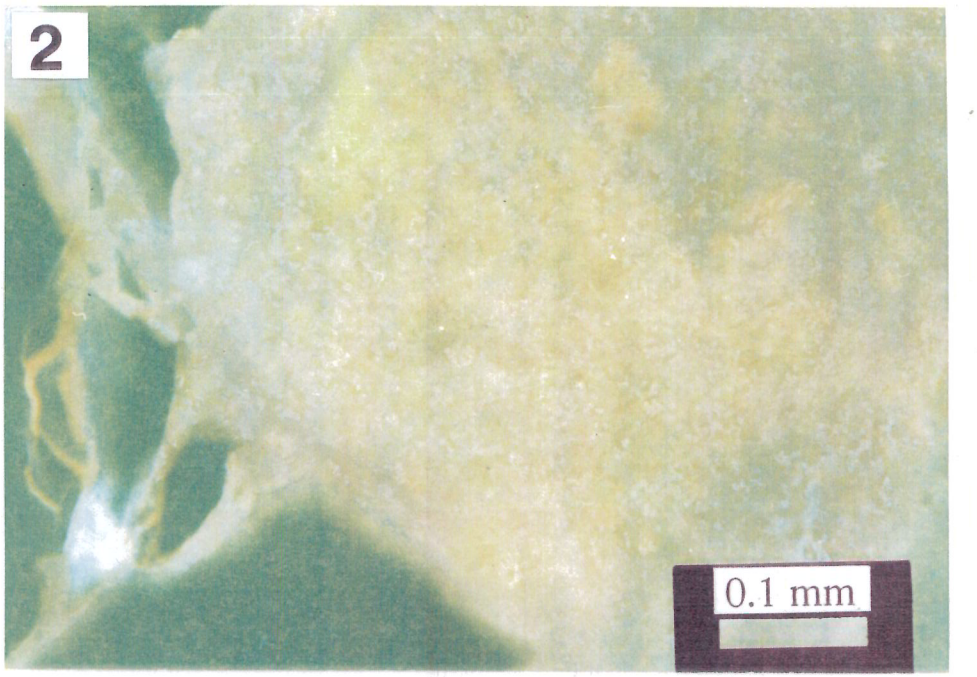
2
0.1 mm

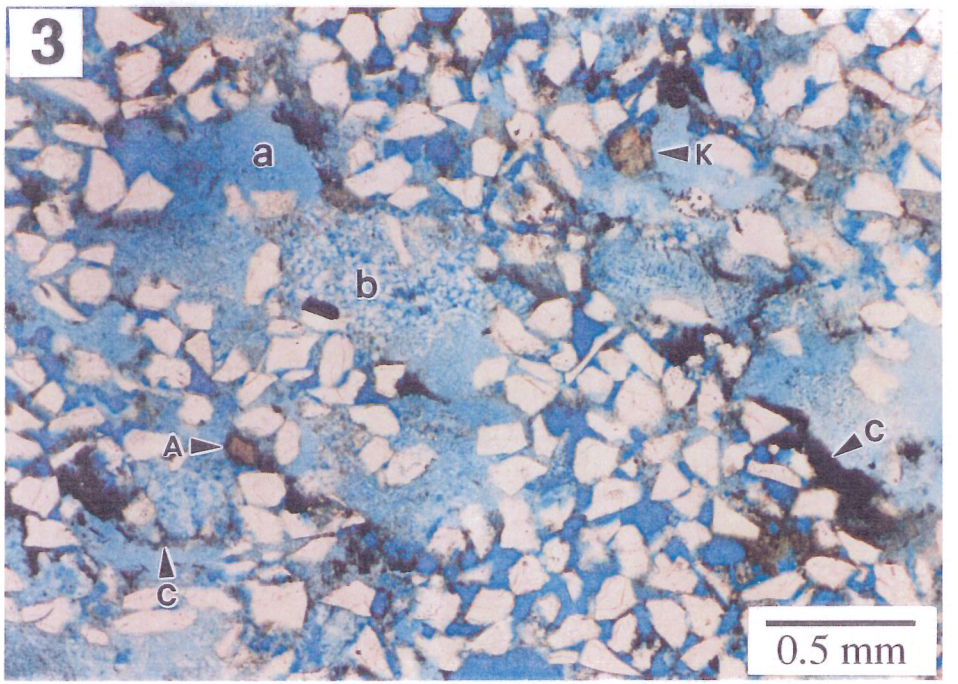
3
a
K
b
A
c
c
0.5 mm

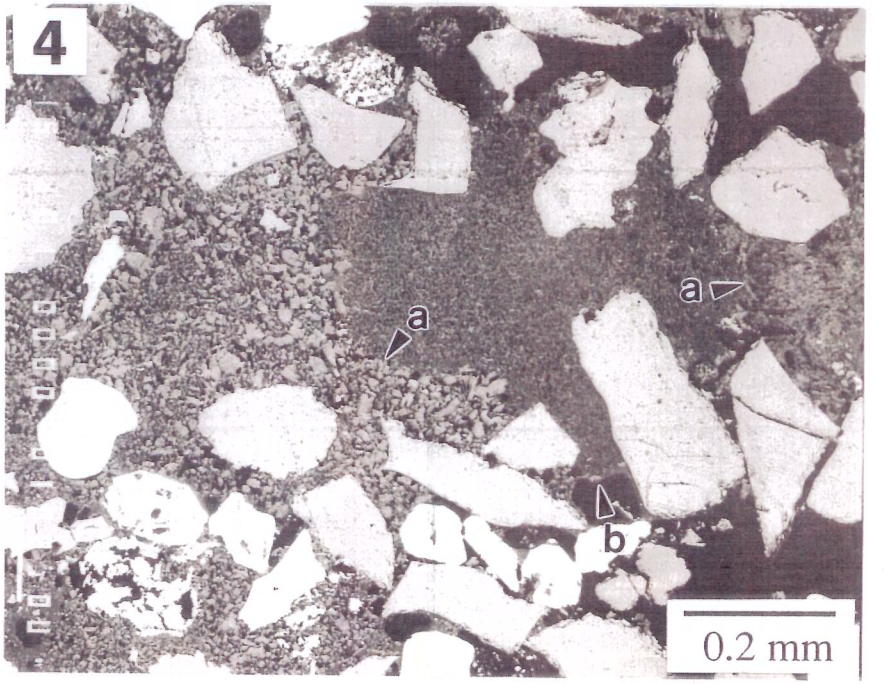
4
a
a
b
0.2 mm

Photo 5. Ione sandstone (#89-09), Apricum Hill, Ione (PPL). View shows a well sorted, medium-grained Ione sandstone with detrital clasts comprised of quartz (white), kaolinized mica books (KM), K-feldspar (K), zircon (Z), and abundant sand-sized kaolinite aggregates deformed between rigid grains forming pseudomatrix. Adjacent clay aggregate boundaries are delineated by variations in their microfabric and amounts of O-F cement (a), or remnants of O-F cement coatings (b). Compression produced by impinging rigid grains caused swirls or concentric drape lines of O-F cement in the fabric of the adjacent clay aggregate (c). Incompletely altered remnants of the precursor mineral (probably feldspar) are visible in some clay aggregates (d).

Photo 6. Ione sandstone (#89-09), Apricum Hill (BSE). View shows the pedogenic aggregate microfabric typical of sand-sized kaolinite aggregate clasts in Ione sandstones. The aggregate microfabric is comprised of coarse- and fine-grained kaolinite particles (light gray) with amorphous siliceous-rich cement (dark gray). The amorphous cement forms meniscus shaped drapes between the kaolinite particles and commonly entrains spherical microvoids (a) which appear as diffuse O-F cement or discrete opaque particles in the clay fabric (PPL).

Photo 7. Ione sandstone (#92-02), Road outcrop Hwy 124, Ione (PPL with WRL). View shows a Lower Ione sandstone fabric from a weathered road cut exposure. Goethite precipitation (yellow) is associated with the oxidation of O-F cement coatings (a) and O-F concentrations in the fabric of the clay aggregates (b). The arrangement of goethite cement occurring in the clay aggregate fabric appears related to variations in the amount and arrangement of precursor O-F cement (organo-siliceous) in the clay aggregates. Compare patterns of goethite cement at "a and b" with arrangement of O-F cement in clay aggregates in Photo 5, "b and c".

Photo 8. Ione sandstone (#89-13), mottled horizon in the paleosol at Apricum Hill (PPL with WRL). View shows iron oxide precipitation in a quartzose Lower Ione sandstone. Most of the kaolinite matrix is associated with goethite precipitation (yellow). Hematite precipitation (red) is randomly distributed in the kaolinite fabric but sometimes associated with laminae concentrated with heavy minerals. Amphibole grains (A) show little or no effects of dissolution and many do not exhibit oxidation halos. This thin section was impregnated with colorless epoxy.

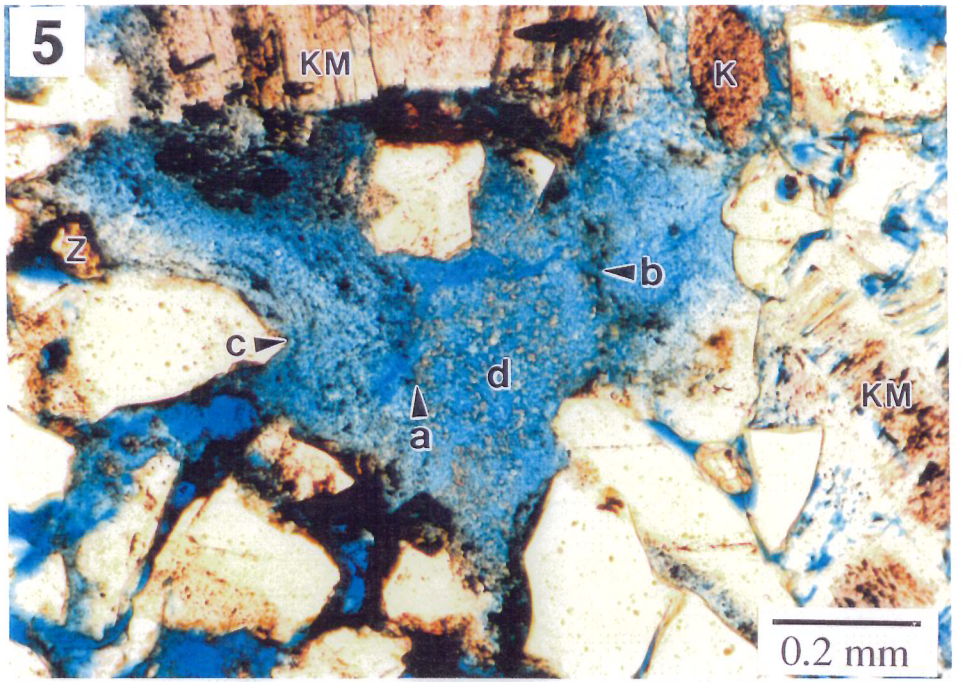
5
KM
K
Z
b
c
d
a
KM
0.2 mm

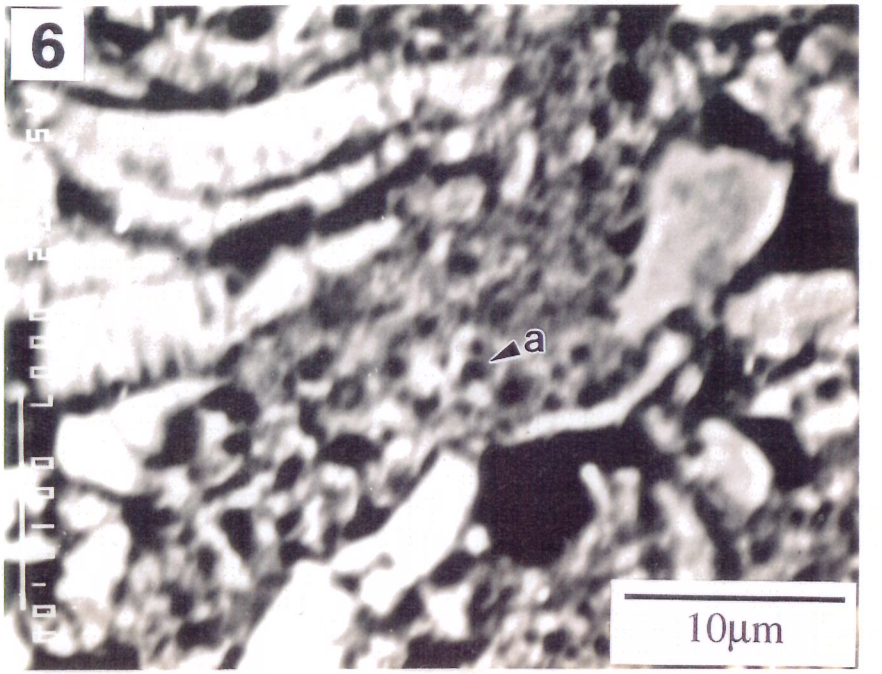
6
a
10μm

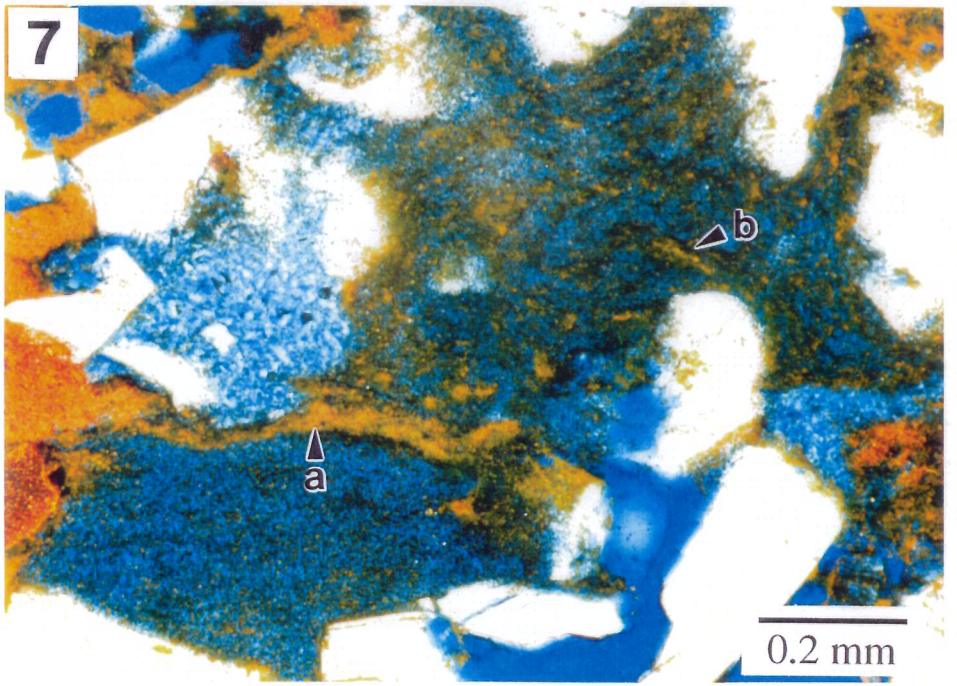
7
b
a
0.2 mm

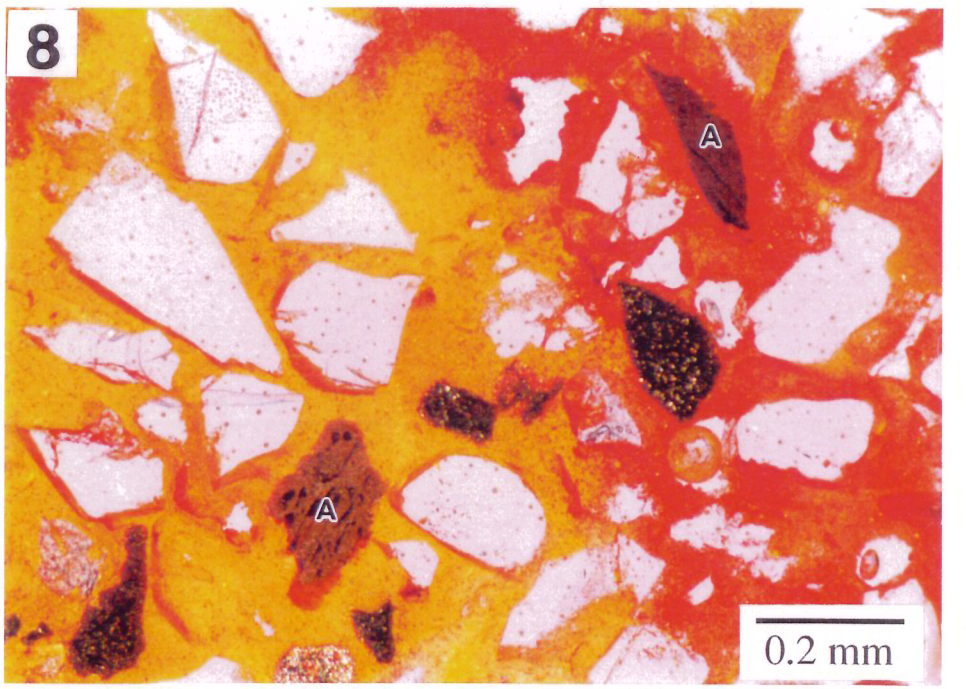
8
A
A
0.2 mm